JOC Article

Ab Initio Evaluation of Intramolecular Electron Transfer Reactions in Halobenzenes and Stabilized Derivatives

Adriana B. Pierini* and D. Mariano A. Vera

INFIQC, Departamento de Química Orgánica, Facultad de Ciencias Químicas, Universidad Nacional de Córdoba, 5000 Córdoba, Argentina

adriana@dqo.fcq.unc.edu.ar

The potential energy surfaces for the fragmentation of the radical anions of p-nitrochlorobenzene and p- and m-chloroacetophenones were explored using first principle methods. The behavior of these compounds, stabilized by π acceptors, is compared to that shown by the unsubstituted halobenzenes (PhX, X = F, Cl, Br, I). The presence of π and σ radical anions was inspected as well as the intramolecular electron transfer (intra-ET) from the π to the σ surface, responsible for the dissociation of these intermediates. The profiles obtained with the B3LYP functional in the gas phase and in the presence of a polar solvent are in agreement with the spectroscopic evidence and with the experimentally observed reactivity of the compounds under study. The stability of the radical anion of p-nitrochlorobenzene and the adiabatic and endothermic nature of its dissociation are explained. The order of the rate constants for dissociation m-chloroacetophenone < p-chloroacetophenone is interpreted on the basis of the differences in the adiabatic character of the intra-ET of both isomers which is ascribed to the nodal properties of their SOMOs. In the halobenzene family, the electronic factors responsible for the intra-ET are analyzed. The stabilization of the σ surface exerted by the different halogens and its effect on the rate constants for dissociation are explained.

The intermolecular electron transfer (ET) to aliphatic halides follows a concerted-dissociative pathway,[1−3] that is, the C−halogen bond (C−X) breaks as the electron is being transferred. On the other hand, a stepwise mechanism, with formation of radical anions as intermediates, is the preferred pathway followed in the ET to a halide bearing a π acceptor of low enough energy to accommodate the incoming electron (eq 1).[1,3−5] The presence of radical anions as intermediates has been clearly estab-

lished in many organic reactions.[1,6,7] In these intermediates, the π acceptor can be linked to the C−X bond through a bridge or it can be orthogonal and adjacent to it, as is the case for aromatic halides. For these compounds, two different anionic surfaces are a priori possible, one corresponding to a radical anion in which the extra electron is located on the π system (π RA) and the other corresponding to a σ* C−halogen radical anion (σ RA). Despite the fact that the σ surface is proposed as dissociative,[8a] this meaning that no minimum is expected on this surface with the exception of a possible shallow one corresponding to a loose R•X− complex,[1] the existence of σ intermediates has been estimated on spectroscopic[9] and theoretical[10] bases for different systems. When a

* Author to whom correspondence may be addressed. Fax: 54-351-4333030/4334174. Phones: 54-351-4334170/73.

(1) Savéant, J.-M. *Adv. Phys. Org. Chem.* Tidwell, T. T., Ed.; Academic Press: New York, 2000; p 35.

(2) For references related to ET to aliphatic halides in the gas phase and in apolar or weakly polar matrices, see: (a) Compton, R. G.; Reinhart, P. W.; Cooper, C. C. *J. Chem. Phys.* **1978**, *68*, 4360. (b) Symons, M. C. R. *Pure Appl. Chem.* **1981**, *53*, 223. (c) Hasegawa, A.; Williams, S. *Chem. Phys. Lett.* **1977**, *46*, 66. (d) Hasegawa, A.; Shiatani, M.; Williams, S. *Faraday Discuss.* **1977**, 157. (e) Kuhn, A.; Illenberger, E. *J. Phys. Chem.* **1989**, *93*, 7060. (f) Kuhn, A.; Illenberger, E. *J. Chem. Phys.* **1990**, *93*, 357.

(3) For electrochemical reduction of aliphatic and aromatic halides, see: (a) Savéant, J.-M. *Adv. Phys. Org. Chem.* **1990**, *26*, 1. (b) Andrieux, C. P.; Gallardo, I.; Savéant, J.-M.; Su, K. B. *J. Am. Chem. Soc.* **1986**, *108*, 638. (c) Andrieux, C. P.; Gallardo, I.; Savéant, J.-M.; Su, K. B. *J. Phys. Chem.* **1986**, *90*, 3815. (d) Andrieux, C. P.; Merz, A.; Savéant, J.-M. *J. Am. Chem. Soc.* **1985**, *107*, 6097. (e) Andrieux, C. P.; Gélis, L.; Médebielle, M.; Pinson, J.; Savéant, J.-M. *J. Am. Chem. Soc.* **1990**, *112*, 3509.

(4) (a) Wentworth, W. E.; Becker, R. S.; Tung, R. *J. Phys. Chem.* **1967**, *71*, 1652. (b) Steelhammer, J. C.; Wentworth, W. E. *J. Chem Phys.* **1969**, *51*, 1802.

(5) (a) Hawley, M. D. In *Encyclopedia of the Electrochemistry of the Elements*; Bard, A. J., Lund, H., Eds.; Wiley: New York, 1980; Vol XIV, Organic Section. (b) Becker, J. Y. In *The Chemistry of Functional Groups, Supplement D*; Patai, S., Rappoport, Z., Eds; Wiley: New York, 1983; Chapter 6, p 203.

(6) (a) Rossi, R. A.; Peñéñory, A. B.; Pierini A. B. *Chem. Rev.* **2003**, *103*, 71. (b) Rossi, R. A.; Pierini, A. B.; Peñéñory, A. B. In *The Chemistry of Functional Groups, Supplement D2*; Patai, S., Rappoport, Z., Eds.; Wiley: Chichester, 1995; Ch 24, p 1395. (c) Rossi, R. A.; Pierini, A. B.; Santiago, A. N. In *Organic Reactions*; Paquette, L. A., Bittman, R., Eds.; John Wiley & Sons: New York, 1999; p 1.

(7) (a) Andrieux, C. P.; Robert, M.; Saeva, F. D.; Savéant, J.-M. *J. Am. Chem. Soc.* **1994**, *116*, 7864. (b) Andrieux, C. P.; Savéant, J.-M.; Tardy, C. *J. Am. Chem. Soc.* **1997**, *119*, 11546. (c) Severin, M. G.; Farnia, G.; Vianello, E.; Arévalo, M. C. *J. Electroanal. Chem.* **1988**, *251*, 369. (d) Jakobsen, S.; Jensen, H.; Pedersen, S. U.; Daasbjerg, K. *J. Phys. Chem. A* **1999**, *103*, 4141. (e) Antonello, S.; Maran, F. *J. Am. Chem. Soc.* **1997**, *119*, 12595. (f) Daasbjerg, K.; Jensen, H.; Benassi, R.; Taddei, F.; Antonello, S.; Gennaro, A.; Maran, F. *J. Am. Chem. Soc.* **1999**, *121*, 1750. (g) Costentin, C.; Hapiot, P.; Médebielle, M.; Savéant, J.-M. *J. Am. Chem. Soc.* **1999**, *121*, 4451. (h) Pause, L.; Robert, M.; Savéant, J.-M. *J. Am. Chem. Soc.* **1999**, *121*, 7158. (i) Speiser, B. *Angew. Chem., Int. Ed. Engl.* **1996**, *35*, 2471. (j) Pause, L.; Robert, M.; Savéant, J.-M. *J. Am. Chem. Soc.* **2001**, *123*, 4886.

(8) (a) Clarke, D. D.; Coulson, C. A. *J. Chem. Soc. A* **1969**, 169. (b) Dressler, R.; Allan, M.; Haselbach, E. *Chimia* **1985**, *39*, 385.

minimum is located on both surfaces, the species can be characterized as orbital or electronic isomers,[11] since they differ in energy, geometry, and their orbital occupancy (i.e., SOMO on the aromatic system or in the σ breaking bond).

$$RX + e \rightleftharpoons (RX)^{\bullet-} \qquad (1)$$

$$(RX)^{\bullet-} \rightarrow R^{\bullet} + X^{-} \qquad (2)$$

The intramolecular ET (intra-ET) from the π system to the σ^* C–X bond is the necessary condition for dissociation of the π intermediate in the sense of eq 2.[1] Only the σ species cleaves into a radical and the halide ion,[8a] while the π potential surface correlates with the halogen atom loss.[8] At the geometry of their crossing, the π and σ states are electronically uncoupled due to symmetry reasons.[12–14] However, they become coupled, the crossing is avoided, and the intra-ET becomes feasible when the symmetry constraint is released, which can be achieved by bending of the C–halogen bond with respect to the aromatic ring.[15] Under these conditions, the intra-ET associated with the crossing of both surfaces can be diabatic or adiabatic, the latter when a considerable π–σ coupling occurs.[8,14,16]

The relative energy of the π and σ surfaces depends on molecular factors such as the energy of the π LUMO and the dissociation energy of the C–X bond, in other words, the energy of the σ^* C–X MO.[1]

The energy of the (RX + e) curve with respect to the anionic surfaces can be addressed in the gas phase by either theoretical or experimental means.[8,10,17,18] The energy gap to the π anionic curve at the geometry of the neutral (vertical electron affinity) is accessible form scattering data;[8b,19] their relative energy is dependent on molecular factors. For example, the π anionic surface of halobenzenes, compounds with negative electron affinity (EAs computed as $E(ArX) - E(ArX^{\bullet-})$), lies at a higher energy than the neutral. Halobenzenes substituted by π acceptors are characterized by a positive EA, and their π anionic surface lies at a lower energy than the neutral.
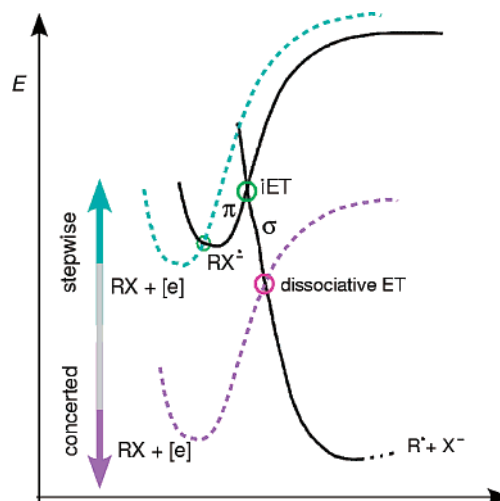

FIGURE 1. Schematic profiles for the ET to a haloaromatic or haloaliphatic compound with a π acceptor. For a given RX, the reaction can switch from stepwise to dissociative by driving force modifications.

The energetics of the (RX + e) and the σ (R$^{\bullet}$ + X^{-}) surfaces are revealed in thermal dissociative electron attachment experiments and can be predicted either by electronic structure calculations or from empirical potentials.[10,17,18,19]

The anionic–neutral energy ordering can be modified by the presence of a third body, as for example solvent molecules. In this medium, the energy of the (RX + e) surface also depends on the experimental conditions used to perform the ET. Interestingly, a transition from a stepwise to a concerted mechanism has been shown to be possible by changing the driving force of the experimental conditions, which ultimately modifies the energy of the (RX + e) surface. This mechanistic switch can be achieved photochemically,[7j] electrochemically (by changing for example, the electrode potential), and in a bimolecular homogeneous ET, by modifying the reduction potential of the donor. The general situation is schematically shown in Figure 1.[1,7]

Radical anions have been the subject of theoretical studies due to their importance in different types of organic reactions including DNA damage.[20–22] Our main interest is the interpretation of the electronic properties related to their chemical reactivity.[15,21] For this reason, we present here a DFT[23] study for the radical anions of halobenzenes (PhX, X = F, Cl, Br, I) and for *p*- and *m*-chloroacetophenones and *p*-nitrochlorobenzene in the gas phase and in a polar solvent. These compounds were

(9) (a) Symons, M. C. R. *J. Chem. Soc., Chem. Commun.* **1977**, 408. (b) Symons, M. C. R. *J. Chem. Soc., Faraday Trans. 1* **1981**, *77*, 783. (c) Symons, M. C. R.; Bowman, W. R. *J. Chem. Soc., Perkin Trans. 2* **1990**, 975.

(10) (a) Clark, T. *J. Chem. Soc., Chem. Commun.* **1981**, 515; **1984**, 93. (b) Clark, T.; Illing, G. *J. Chem. Soc., Chem. Commun.* **1985**, 529. (c) Betran, J.; Gallardo, I.; Moreno, M.; Savéant, J.-M. *J. Am. Chem. Soc.* **1992**, *114*, 9576.

(11) (a) Dewar, M. J. S.; Kirschner, S.; Kollmar, H. W. *J. Am. Chem. Soc.* **1974**, *96*, 5242. (b) Dewar, M. J. S.; Pakiari, A. H.; Pierini, A. B. *J. Am. Chem. Soc.* **1982**, *104*, 3242.

(12) (a) Hegarty, D.; Robb, M. A. *Mol. Phys.* **1979**, *83*, 1975. (b) Eade, R. H. E.; Robb, M. A. *Chem. Phys. Lett.* **1981**, *83*, 362.

(13) (a) Bearpark, M. J.; Robb, M. A.; Schlegel, H. B. *Chem. Phys. Lett.* **1994**, *223*, 269. (b) Ragazos, I. N.; Robb, M. A.; Bernardini, F.; Olivucci, M. *Chem. Phys. Lett.* **1992**, *197*, 217.

(14) Salem, L. In *Electrons in Chemical Reactions: First Principles*; John Wiley & Sons: New York, 1982; Ch. 4–5.

(15) (a) Pierini, A. B.; Duca, J. S., Jr. *J. Chem. Soc., Perkin Trans. 2* **1995**, 1821. (b) Pierini, A. B.; Duca, J. S., Jr.; Vera, D. M. A. *J. Chem. Soc., Perkin Trans. 2* **1999**, 1003.

(16) Newton, M. D. *Chem. Rev.* **1991**, *91*, 767.

(17) (a) German, E. D.; Kuznetsov, A. M *J. Phys. Chem.* **1995**, *99*, 9095. (b) Costentin, C.; Robert, M.; Savéant, J.-M. *J. Am. Chem. Soc.* **2003**, *125*, 105.

(18) Marcus, R. A. *Acta Chem. Scand.* **1998**, *52*, 858.

(19) (a) Jordan, K. D.; Burrow, P. D. *Chem. Rev.* **1987**, *87*, 557. (b) Jordan, K. D.; Burrow, P. D. *Acc. Chem. Res.* **1978**, *11*, 341. (c) Kebarle, P.; Chowdhury, S. *Chem. Rev.* **1987**, *87*, 513.

(20) (a) Borosky, G. L.; Nishimoto, S.-I.; Pierini, A. B. *THEOCHEM* **2000**, *499*, 151. (b) Sommerfeld, T. *ChemPhysChem.* **2000**, *11*, 677. (c) Wetmore, S. D.; Boyd, R. J.; Eriksson, L. A. *Chem. Phys. Lett.* **2001**, *343*, 151. (d) Laage, D.; Burghart, I.; Sommerfeld, T.; Hynes, J. T. *ChemPhysChem.* **2003**, *4*, 61.

(21) (a) Vera, D. M. A. Computational Chemistry and its application to electron transfer processes in organic systems. Ph.D. Thesis, Universidad Nacional de Córdoba, 2001. (b) Vera, D. M. A.; Pierini, A. B. *J. Phys. Org. Chem.* **2002**, *15*, 894.

(22) (a) Beregovaya, I. V.; Shchegoleva, L. N. *Chem. Phys. Lett.* **2001**, *348*, 501. (b) Benassi, R.; Bernardi, F.; Botonni, A.; Robb, M. A.; Taddei, F. *Chem. Phys. Lett.* **1989**, *161*, 79. (c) Konovalov, V. V.; Laev, S. S.; Beregovaya, I. V.; Shchegoleva, L. N.; Shteingarts, V. D.; Tsvetkov, Y. D.; Bilkis, I. *J. Phys. Chem. A* **2000**, *104*, 352.

(23) (a) Hohenberg, P.; Kohn, W. *Phys. Rev.* **1964**, *136*, B864. (b) Kohn, W.; Sham, I. J. *Phys. Rev.* **1965**, *140*, A1133.

chosen in order to determine, for a given π system, the effect of different halogens that influences the energy of the σ surface. For a given halogen, the effect of π systems with a different degree of stabilization and the effect of their position on the aromatic ring were also inspected.

This study, which includes σ and π effects, could allow the understanding of the dissociation and the rationalization of the chemical behavior of radical anions in processes in which we are experimentally concerned, such as the $S_{RN}1$ mechanism.[6]

Computational Procedure

The calculations were performed with the Gaussian98 packages of programs.[24] The characterization of stationary points was done as usual by Hessian matrix calculations.[25] In most cases, a preliminary inspection of the potential surfaces was carried at the unrestricted Hartree−Fock (UHF) level. Afterward, their exploration within the B3LYP[26] DFT[23] functional was performed varying the selected coordinate with full geometry optimization for the remainder degrees of freedom. In all cases, the B3LYP spin contamination along the whole fragmentation path was negligible ($\langle S^2 \rangle = 0.750-0.751$).

For key thermodynamic quantities, the zero-point energy corrections were made at the 6-31G* level. To compare the thermochemistry predicted by different levels of theory and for the different halides, the relative energy (E_{rel}) of any structure is given with respect to the dissociated fragments R$\cdot$ + X$^-$ (E_{rel}(R$\cdot$+X$^-$) = 0, by definition). The effect of acetonitrile (MeCN) as a polar solvent was evaluated through the Tomasi's polarized continuum model (PCM and IPCM)[27] as implemented in Gaussian98. For the stabilized derivatives, these calculations were performed with full geometry optimization from the gas-phase structures. For the halobenzenes, which fragment through a more exothermic path, the σ species were calculated at the gas-phase geometry.

At the geometry near the neutral molecule, the gas-phase anionic state of halobenzenes, compounds characterized by their negative EAs, lies at higher energies than the neutral state and so the anion is unstable with respect to the spontaneous electron detachment. In this

family, and due to difficulties of ab initio methods in dealing with these species,[28] the potential surfaces obtained were checked against different sources of experimental information (see below). However, the gas-phase instability of these anions is unimportant in organic reactions in a polar solvent, since in this medium, the anionic states lie below the neutrals. Besides, our study includes only conventional valence anion states.

A reasonably good agreement was obtained for PhX (X = Cl, Br) by using either the 6-31G*, the 6-31+G*, or the 6-311+G(2d,p) basis.[29] Only the last two yielded almost the same results for X = F. Even though the ECP LANL2DZ is expected to be of lower quality than the basis used for most calculations, its was included to count with an intermediate quality basis for the whole series of halides including iodine.

For comparison purposes, MP2 (PMP2/6-31G* and PMP2/6-31+G*), CCD, CCSD, and CCSD(T)/6-31+G* calculations were carried out for PhCl (see Supporting Information); the Moeller−Plesset results were not better than those of B3LYP with the same basis. This functional gives results in reasonably good agreement with the highest level of coupled cluster[30] used.

For the PhX family, the multiconfigurational SCF procedure CASSCF in the (9,8) subspace (nine electrons in eight active MOs) with the 6-31G* and 6-31+G* basis sets was used in order to characterize the low-lying π^* excited state that participates with the anionic π ground state in the intra-ET. The vertical energy gap between the π and π^* states was obtained from the state-averaged calculation using equal weighting factors for both states. This calculation yields the energy of the lowest excited state at the anionic ground-state geometry. The geometry at the crossing point between both π-type states was located by using the keyword Opt=Conical, to find the point for which the energy separation between the two states involved is minimal. At this point, the nonadiabatic coupling was estimated as twice the energy gap (indicated as 2Δ in Figure 7).[12,13] The 8 MO subspace includes two pairs of π/π^* MOs of b_1 symmetry, one pair of π/π^* of a_2 symmetry, and the σ/σ^*C−halogen pair of MOs (a_1 symmetry).

Results and Discussion

Stabilized Systems. The most stable anionic species of p- and m-chloroacetophenone and p-nitrochlorobenzene are of π type and lie at similar and lower energy than the neutrals, respectively (i.e., positive electron affini-

(24) Frisch, M. J.; Trucks, G. W.; Schlegel, H. B.; Scuseria, G. E.; Robb, M. A.; Cheeseman, J. R.; Zakrzewski, V. G.; Montgomery, J. A., Jr.; Stratmann, R. E.; Burant, J. C.; Dapprich, S.; Millam, J. M.; Daniels, A. D.; Kudin, K. N.; Strain, M. C.; Farkas, O.; Tomasi, J.; Barone, V.; Cossi, M.; Cammi, R.; Mennucci, B.; Pomelli, C.; Adamo, C.; Clifford, S.; Ochterski, J.; Petersson, G. A.; Ayala, P. Y.; Cui, Q.; Morokuma, K.; Malick, D. K.; Rabuck, A. D.; Raghavachari, K.; Foresman, J. B.; Cioslowski, J.; Ortiz, J. V.; Stefanov, B. B.; Liu, G.; Liashenko, A.; Piskorz, P.; Komaromi, I.; Gomperts, R.; Martin, R. L.; Fox, D. J.; Keith, T.; Al-Laham, M. A.; Peng, C. Y.; Nanayakkara, A.; Gonzalez, C.; Challacombe, M.; Gill, P. M. W.; Johnson, B. G.; Chen, W.; Wong, M. W.; Andres, J. L.; Head-Gordon, M.; Replogle, E. S.; Pople, J. A. *Gaussian 98*, revision A.7; Gaussian, Inc.: Pittsburgh, PA, 1998.

(25) When different electronic configurations are possible, the different anionic states are selected by giving the right initial guess using the keyword "Guess=Alter", further proceeding with the checking of their stability and characterization. All these DFT results were checked with CASSCF procedure and also with electron-scattering data.

(26) (a) Lee, C.; Yang, W.; Parr, R. G. *Phys. Rev. B* **1988**, *37*, 785. (b) Becke, A. D. *Phys. Rev. A* **1988**, *38*, 3098. (c) Miehlich, B.; Savin, A.; Stoll, H.; Preuss, H. *Chem. Phys. Lett.* **1989**, *157*, 200.

(27) (a) Miertus, S.; Scrocco, E.; Tomasi, J. *Chem. Phys.* **1981**, *55*, 117. (b) Miertus, S.; Tomasi, J. *Chem. Phys.* **1982**, *65*, 239. (c) Cossi, M.; Barone, V.; Cammi, R.; Tomasi, J. *Chem. Phys. Lett.* **1996**, *255*, 327.

(28) (a) Ahlrichs, R. *Chem. Phys. Lett.* **1975**, *34*, 570. (b) Simons, J.; Jordan, K. D. *Chem. Rev.* **1987**, *87*, 535. (c) Simons, J. *J. Chem. Phys.* **1981**, *75*, 2465. (d) Chen, C.-S.; Feng, T.-H.; Chao, J. S.-Y. *J. Phys. Chem.* **1995***, 99*, 8629. (e) Falcetta, M. F.; Choi, Y.; Jordan, K. D. *J. Phys. Chem. A* **2000**, *104*, 9605. (f) Falcetta, M. F.; Jordan, K. *J. Phys. Chem.* **1990**, *94*, 5666. (g) Rescigno, T. N.; Orel, A. E. *J. Phys. Chem.* **1980**, *73*, 6347. (h) Chao, J. S.-Y. *J. Phys. Chem.* **1993**, *97*, 4016. (i) Chao, J. S.-Y. *Chem. Phys. Lett.* **1991**, *179*, 169.

(29) Triple-ζ basis for bromine and third-row elements are available in Gaussian 98: (a) Binning, R. B., Jr.; Curtiss, L. A. *J. Comput. Chem.* **1990**, *11*, 1206. (b) Curtiss, L. A.; McGrath, M. P.; Blaudeau, J.-P.; Davis, N. E.; Binning R. C., Jr.; Radom, L. *J. Chem. Phys.* **1995**, *103*, 6104. (c) McGrath, M. P.; Radom, L. *J. Chem. Phys.* **1991**, *94*, 511.

(30) (a) Pople, J. A.; Krishnan, R.; Schlegel, H. B.; Binkley, J. S. *Int. J. Quantum Chem. Symp.* **1978**, *XIV*, 545. (b) Purvis, G. D.; Bartlett, R. J. *J. Chem. Phys.* **1982**, *76*, 1910. (c) Scuseria, G. E.; Janssen, C. L.; Schaefer, H.F., III. *J. Chem. Phys.* **1988**, *89*, 7382. (d) Scuseria, G. E.; Schaefer, H. F., III. *J. Chem. Phys.* **1989**, *90*, 3700.

TABLE 1. Systems Containing Stabilized π Systems. B3LYP Main Stationary Points Including Solvent Effect[a]

| | gas phase | | | | acetonitrile[b] | |
	6-31G* r(C−Cl)/Å	E_{rel}	6-31+G* E_{rel}	6-311+G(2d,p) E_{rel}	r(C−Cl)/Å	E_{rel}
			p-Nitrochlorobenzene			
neutral molecule	1.751	−17.11	−2.79	−4.22		
π RA	1.784	−38.71	−38.26	−39.36	1.772	−79.52
σ RA					2.757	−66.21
products (Ar• + Cl⁻)	∞	0.00	0.00	0.00	∞	−67.32
			p-Chloroacetophenone			
neutral molecule	1.755	−17.55	−3.11	−4.54		
π RA	1.789	−21.46	−18.73	−20.71	1.779	−59.41
σ RA					2.885	−63.94
products (Ar• + Cl⁻)	∞	0.00	0.00	0.00	∞	−66.75
			m-Chloroacetophenone			
neutral molecule	1.760	−17.12	−3.04	−3.98		
π RA	1.803	−22.16	−19.58	−21.56	1.794	−60.07
σ RA	2.650	−15.24	−11.19	−11.87	3.115	−63.78
products (Ar• + Cl⁻)	∞	0.00	0.00	0.00	∞	−66.65

[a] Relative energy is in kcal/mol defined with respect to the gas-phase fragmentation products Ar• + Cl⁻. Both gas phase and solvated species have zero-point corrections at the B3LYP/6-31G* level. [b] PCM, B3LYP/6-31G* with complete geometry optimization from the gas-phase structures.
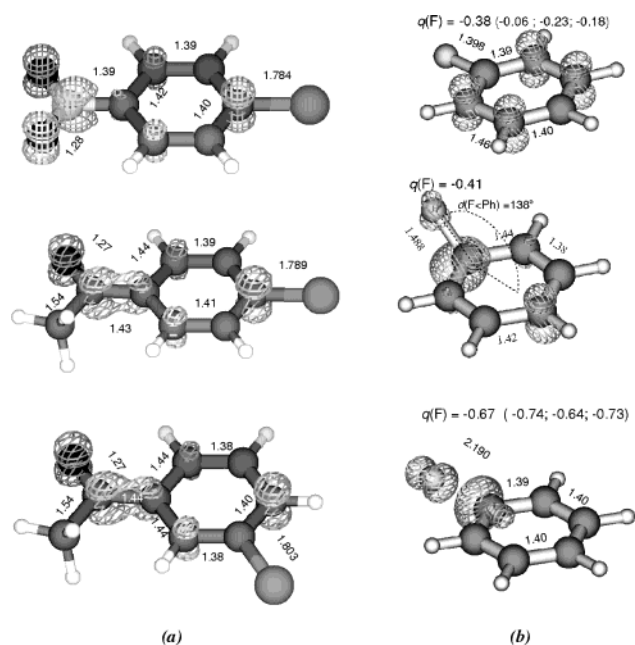

FIGURE 2. (a) From top to bottom main features of the stable π RAs of *p*-nitrochlorobenzene and *p*- and *m*-chloroacetophenone. (b) B3LYP/6-31+G* RAs of PhF: spin density, main geometric parameters, and charge on fluorine (in parentheses are the charges for X = Cl, Br, and I, respectively).

ties).[31] The π RA of the nitro derivative can be taken as a paradigmatic example of a very stable and long-lived anionic intermediate which is ≈38 kcal/mol more stable than the dissociation fragments. The main geometric parameters and unpaired spin density distribution of these RAs are shown in Figure 2a. Their relative stability with respect to the dissociated fragments (Ar• + Cl⁻) and their C−Cl bond distances are presented in Table 1. As can be seen in the figure, the *p*-NO₂C₆H₄Cl π RA has ~63% of the unpaired electron located on the NO₂ group, a small negative charge on the halogen, and a shortened C−NO₂ bond length with respect to the neutral. A similar spin distribution, oriented by the electron-withdrawing

group, is shown by the *p*-acetyl derivative. In both para RAs, the main coefficients of their π SOMOs are located on their C_{ipso} (halogen-substituted carbon), on their C_{para}, and on the substituent. At difference with the para derivatives, the SOMO of the *m*-acetyl intermediate is nodal at the C_{ipso}, which bears no spin density.

The ²B₁ π RA of *p*-nitrochlorobenzene, SOMO without a C_{ipso} node, gradually transforms into σ. In this intermediate, the intra-ET occurs through an avoided π−σ crossing mediated by the C−Cl bending with respect to the phenyl ring. This bending allows for an important coupling between the π and the σ^* C−Cl systems, otherwise orthogonal (Figure 3). The intermediate thus fragments adiabatically through a considerably endothermic pathway, which can be followed by inspection of either its SOMO or the spin density, which gradually relocates as the charge is being transferred (see Figure 3). The π RA of *p*-chloroacetophenone transforms into a σ species, following a path similar to that observed for *p*-nitrochlorobenzene RA; the main difference is that the *p*-nitro was found to be ~19 kcal/mol more stable toward dissociation than the *p*-acetyl intermediate.

Although the thermodynamics for dissociation of the *m*- and *p*-acetyl RAs are similar (Table 1), they behave quite differently in the π−σ crossing zone (at ca. 2.1− 2.5 Å), as compared in parts a and b of Figure 4. For the meta compound, the crossing takes place at higher energy, a slightly longer C−Cl distance and through a less adiabatic process than for the para isomer. This behavior is attributed to the C_{ipso} node of the *m*-acetyl SOMO. In agreement with the poorer π−σ coupling observed for the intra-ET of *m*-chloroacetophenone RA, its cleavage has been determined to be >20 times slower than that of its para isomer.[32]

---

(31) Even though the energy of the anionic π and σ surfaces does not vary sensitively going beyond the 6-31*G basis, the EAs, which depend on the neutral and anionic energy difference, have been sensitively improved by inclusion of diffuse functions. The thermal electron affinity of the *m*-chloroacetophenone is calculated to be 0.68 eV (B3LYP/6-31+G*), close to the 0.62 experimental value; the nitro derivative has an even more positive EA of 1.3 eV. See: Mishima, M.; Huh, C.; Lee, H. W.; Nakamura, H.; Fujio, M.; Tsuno, Y. *Tetrahedron Lett.* **1995**, *36*, 2265.
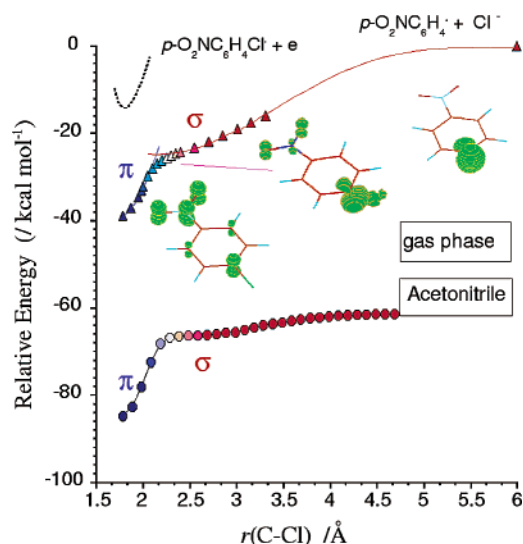
FIGURE 3. B3LYP/6-31G* profiles of *p*-chloronitrobenzene RA in the gas phase and by simulating MeCN. The spin density distribution diagrams at the $^2B_1$ RA, at the $\pi-\sigma$ interconversion region, and at long C−Cl distance are shown.
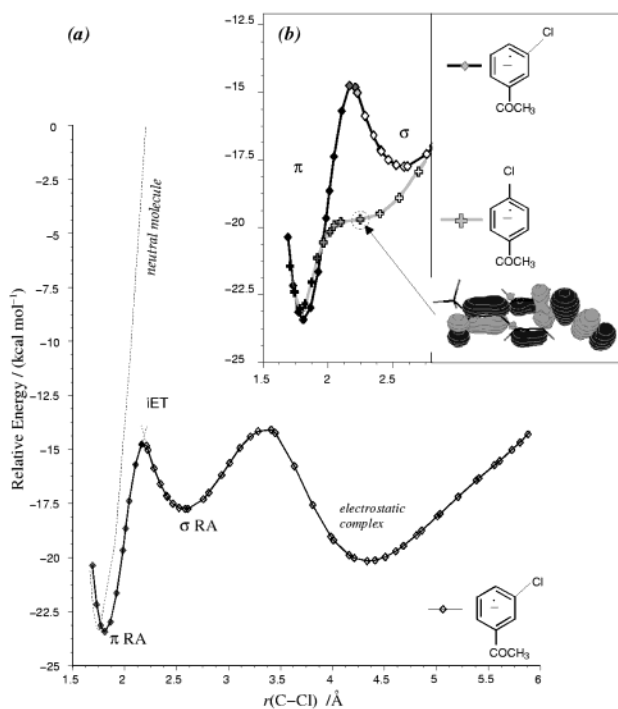

FIGURE 4. (a) B3LYP/3-21G* potential energy surface profiles for the fragmentation of the *m*-chloroacetophenone RA. (b) Comparison of the $\pi-\sigma$ intra-ET zone for the *m*-and *p*-acetyl derivatives.

With respect to the σ surface, an intermediate was located only on the surface of the *m*-acetyl derivative; it has an elongated C−Cl length, most of the negative charge on the halogen and the unpaired spin density on C_{ipso}. This intermediate could not be characterized for the *p*-acetyl isomer mainly because it has coordinates and energy similar to the crossing zone. Despite this fact, the σ surface of both acetyl isomers transforms into a loose electrostatic complex between the radical and the chloride anion. In the gas phase, an important contribution to the

overall barrier for the cleavage of these RAs comes from the separation of the $Ar^{\bullet}X^-$ moieties along the $Ar^{\bullet}\cdots X^-$ curve. However, in MeCN, the electrostatic complexes disappear, the σ RAs are kinetically unimportant, and the fragmentation becomes exothermic (see Table 1). Thus, once the intra-ET to the σ state takes place in a polar solvent, the haloacetophenone RAs dissociate through a downhill path.

On the other hand, the dissociation of the very stable *p*-nitrochlorobenzene RA is still endothermic in solution (Figure 3). Despite the fact that the σ surface and the dissociated fragments suffer the greatest solvent stabilization due to their high charge localization, this stabilization does not suffice to overcome the endothermicity of its dissociation. The profile obtained in Figure 3 is reasonable when compared to the experimentally measured activation energies for *p*-iodo- and *p*-nitrobromobenzene RAs (19−21 kcal/mol).[33] The *p*-nitrochlorobenzene RA does not fragment at an appreciable rate under thermal conditions in MeCN $(k_{frag,thermal} < 10^{-2}\ s^{-1})$ and can fragment through its excited states $(k_{frag,photochem} = 4 \times 10^{-2}\ s^{-1})$; the cleavage is controlled by the $\pi^*-\sigma$ intra-ET.[34,15b]

As expected from the analysis of the calculated surfaces, the chloroacetophenones RAs show an intermediate behavior. They are at least 3 orders of magnitude more reactive toward dissociation than the *p*-nitrochlorobenzene RA, but they dissociate considerably more slowly than the fastest halobenzene family.

Halobenzenes. The general shape of the main anionic profiles obtained for PhCl and the other halobenzenes, together with the potential surface for the C−X bond dissociation of the neutrals, is depicted in Figure 5. As shown in Figure 5a, for all the halides, the lowest π surfaces appear at higher energy than the neutral in agreement with their known negative EAs. At difference with the behavior shown by the stabilized chlorine derivatives, the π surface of PhCl is higher in energy than the σ surface. The same energy ordering is calculated for PhBr and PhI. This ordering is reversed only for PhF. The relative energy of the σ surface with respect to the π one can be roughly rationalized in terms of the properties of the neutral molecules by comparing, along the series, either the C−X bond strength or the energy of the a_1 (σ^*) C−X MO, the first unoccupied orbital with the adequate symmetry for dissociating in the sense of eq 2. The antibonding a_1 (σ^*) C−X MO lies more than 4 eV above the π^* LUMO for X = F, this energy difference sharply decreases to 1.11 and 0.59 eV for X = Cl and X = Br respectively while the a_1 (σ^*) MO becomes the LUMO for X = I (See Supporting Information, Table S2). Thus, while the electron-withdrawing group is responsible for the higher stability of the π RA of p-NO$_2$C$_6$H$_4$Cl in relation to PhCl, the π stability of PhF RA with respect to the σ surface or the dissociated fragments arises from the destabilization of the σ^*(C−F) MO.

The quantities indicated in Figure 5a were used to address the quality of the calculated gas-phase surfaces. The electron affinities of the halogens, EA(X), and bond

(32) Tanner, D. D.; Chen, J. J.; Chen, L.; Luelo, C. *J. Am. Chem. Soc.* **1991**, *113*, 8074.
(33) Parker, V. D. *Acta Chem. Scand.* **1981**, *B35*, 655.
(34) Compton, R. G.; Dryfe, R. A. W.; Fisher, A. C. *J. Chem. Soc., Perkin Trans. 2* **1994**, 1581.
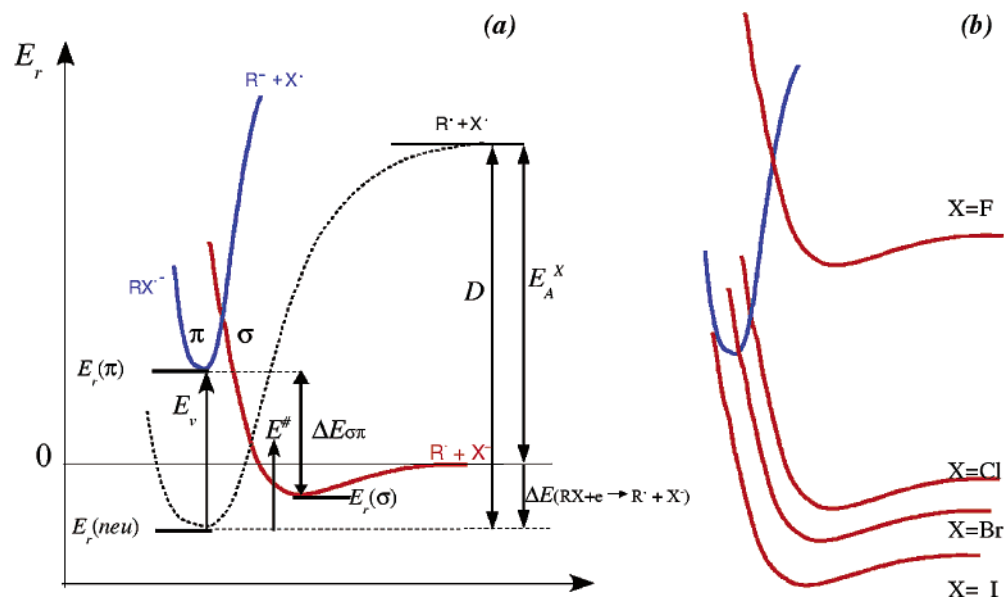
FIGURE 5. Schematic profiles obtained from the DFT scan of the halobenzenes surfaces. (a) General shape and main parameters. (b) Difference in the relative energy of the π and σ anionic profiles in going from X = F, Cl, Br, and I.

TABLE 2. Halobenzenes. Main Stationary Points Including Solvent Effect

		gas phase			acetonitrile[a]
	B3LYP/6-31+G* r(C–Cl)/Å	B3LYP/6-311+G(2d,p) E_{rel}[b]		E_{rel}[b]	E_{rel}[b]
		PhF			
neutral molecule	1.360	−43.63		−45.00	−46.63
$^2A_2$ RA π	1.400	−20.23		−22.62	−73.41
$^2A'$ RA[c]	1.490	−18.18		−19.54	−73.41
$^2A_1$ RA[d] σ	2.190	−11.50		−81.26	−66.21
products (Ph• + F−)	∞	0.00		0.00	−84.83
		PhCl			
neutral molecule	1.760	−5.16		−6.55	−7.70
$^2A_2$ RA π	1.830	−15.91		13.03	−30.42
$^2A_1$ RA σ	2.740	−4.70		−5.46	−58.59
products (Ph• + Cl−)	∞	0.00		0.00	−65.54
		PhBr			
neutral molecule	1.900	−5.89		−3.13	−5.15
$^2A_2$ RA π	1.950	14.14		21.35	−29.92
$^2A_1$ RA σ	2.740	−8.85		−4.92	−59.34
products (Ph• + Br−)	∞	0.00		0.00	−61.46

^{a} Tomasi's polarized continuum model (PCM) energy calculation at the gas-phase structure. B3LYP/6-31+G*. ^{b} As usual, the relative energies are taken with respect to the gas-phase dissociated fragments (Ph• + X−), whose energy is zero by definition. ^{c} The C–F bond forms a 137° angle with the phenyl ring, see Figure 2b. ^{d} Minimum only in the planar (C_{2v}) symmetry space, see Figure 6.

dissociation energies of the neutrals, D, are in good agreement with the experimental thermochemistry for X = F, Cl, and Br (and they are even well reproduced for PhI with the compact LANL2DZ basis).[18,35] The rates (cross sections) and thus the activation energies for the processes of thermal dissociative electron attachment, $E^\#$, as well as their thermodynamics [ΔE(PhX + e → Ph• +X−)] are as expected from the analysis of the potential surfaces obtained.[36] The estimated E_v (the negative vertical electron affinities) are quantitatively in good agreement with electron scattering data, and they are just slightly overestimated.[19,28b,d,37] The calculated values of EA(X), D, $E^\#$, $\Delta E_{\sigma\pi}$, ΔE(PhX + e → Ph•+X−), and E_v,

together with the experimental data available,[35] are collected in Table S2, as Supporting Information. On the basis of these results, the B3LYP functional is shown to be adequate for our purposes. The quantities essential to the present discussion, such as the relative energies of the neutral and anionic species in gas phase and in MeCN, are summarized in Table 2.

At difference with the π RAs of the para-stabilized derivatives, the π RAs of halobenzenes are $^2A_2$ states. These π intermediates have, as previously observed,[15] a C–X distance slightly elongated with respect to the neutral and bond alternancies in the ring (C_{ortho}–C_{meta} bond elongated); the unpaired spin density and the negative charge are mainly delocalized over the ortho and

(35) CRC Handbook of Chemistry and Physics, 1st Student Ed.; Weast, R. C., Ed.; CRC Press: Boca Raton, 1988, and 61st Ed, 1981.
(36) Shimamori, H.; Sunagawa, T.; Ogawa, Y.; Tatsumi, Y. *Chem. Phys. Lett.* **1995**, *232*, 115.

(37) Plot as Supporting Information for PhF, PhCl, and PhBr (Figure S1): correlation coefficient, 0.99987; slope, 1.02; intercept ∼0.2 eV.
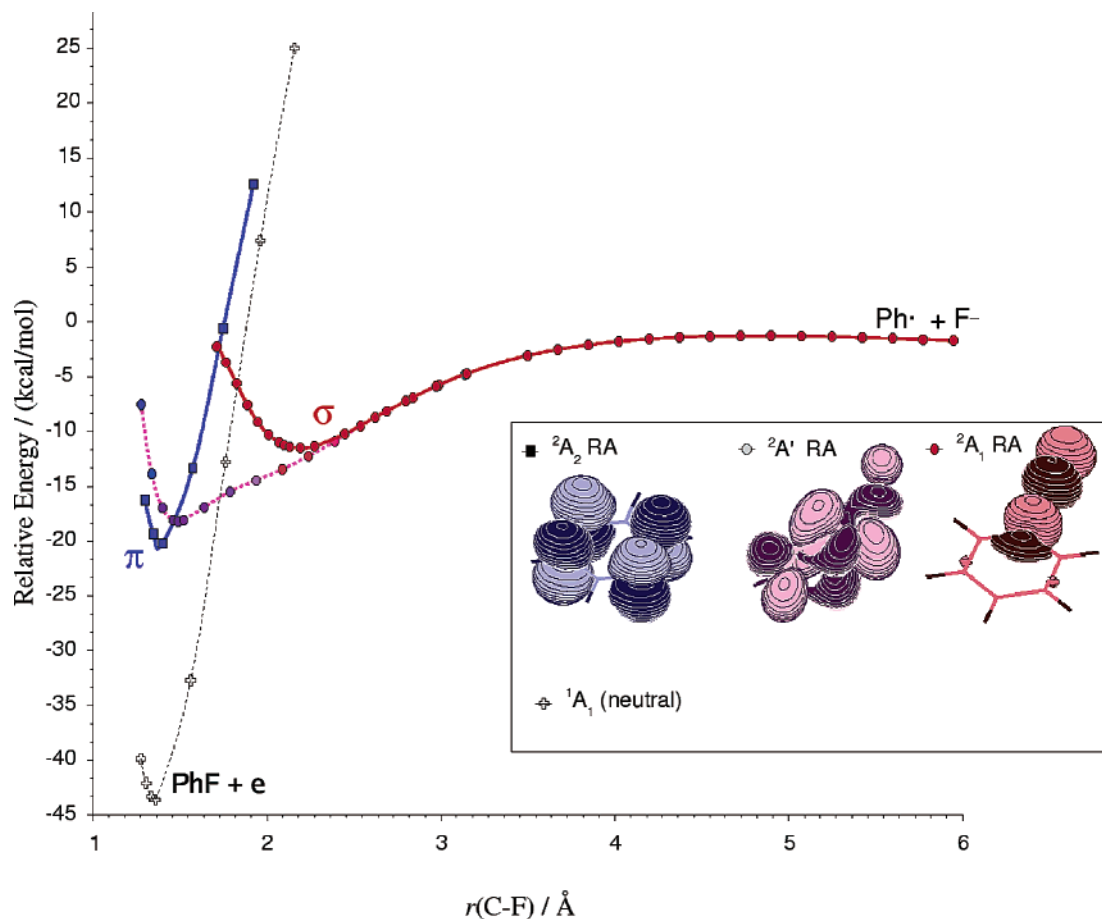
FIGURE 6. B3LYP/6-31+G* surfaces for PhF and its anionic species. The neutral molecule (dotted line), the π $^2A_2$ and σ $^2A_1$ diabatic profiles (line) of the planar species, and the $^2A'$ path (dashed line) in which the planarity is lost. The SOMO diagrams for the relevant anionic species are shown in the bottom right corner.

meta positions as expected from its a_2 SOMO (nodal at the ipso and para carbons) (Figure 2b).

The π ($^2A_2$) and σ ($^2A_1$) surfaces of PhF are shown in Figure 6. A better understanding of the electronic states involved in the intra-ET of the halobenzenes can be obtained by inspecting PhF, mainly due to the stability of its π RA, which is 20.2 kcal/mol with respect to the dissociated fragments (B3LYP/6-31+G*).[38] The modifications produced by changing the halogen to Cl, Br, and I will be presented afterward.

Even though the halogen bending is not relevant for the π–σ coupling in the $^2A_2$ state (SOMO nodal at C_{ipso}), a gradual adiabatic π–σ interconversion path of C_s symmetry, through which the planarity between the phenyl ring and the C–halogen bond is being lost, was found. This is possible due to the existence of an excited π^* $^2B_1$ state, also characterized for the other halobenzenes, which is relatively close in energy to the ground $^2A_2$. The C_{2v} $^2B_1$ state (SOMO without C_{ipso} node) is thus responsible for the b_1 (π^*)–a_1 (σ^*) coupling.

The $^2A'$ minimum located on the C_s curve is predominantly of π character. Its SOMO resembles the b_1 (π^*) orbital but with a C–F contribution due to the loss of planarity (see Figure 2b). This $^2A'$ species gradually becomes σ along the bond-breaking coordinate following an endothermic dissociative path similar to the one observed for the $^2B_1$ (Π) p-NO$_2$C$_6$H$_4$Cl RA. The activation energy to reach the transition state connecting the planar and the bent $^2A'$ minimum was found to be 3.8 kcal/mol (B3LYP/6-31+G*). As for PhF, the C–X bending assists the π–σ intra-ET in PhCl and PhBr RAs by b_1 (π^*)–a_1 (σ^*) mixing. For X = Cl and Br, the σ state is considerably lower in energy than the π one and the $^2A'$ dissociative path is followed downhill collapsing to a much deeper σ minimum as schematically shown in Figure 7 for PhCl. According to B3LYP, the σ surface is even relatively lower in energy for PhI, for which, standing on the equilibrium geometry of the neutral, the first vertical energy leads to the formation of a $^2A_1$ (σ) state.

Further calculations were performed for PhF and PhCl using the multiconfigurational CASSCF(9,8)/6-31+G* procedure. These calculations confirm that the lower anion state of PhF is in fact $^2A_2$ (with CI coefficient of 0.95, for the Slater determinant with the a_2 SOMO). This characterization is in agreement with the first state found by electron scattering[19a,b,28b,d] and with ESR[39] spectroscopy, which predicts for PhF RA an unpaired spin-density
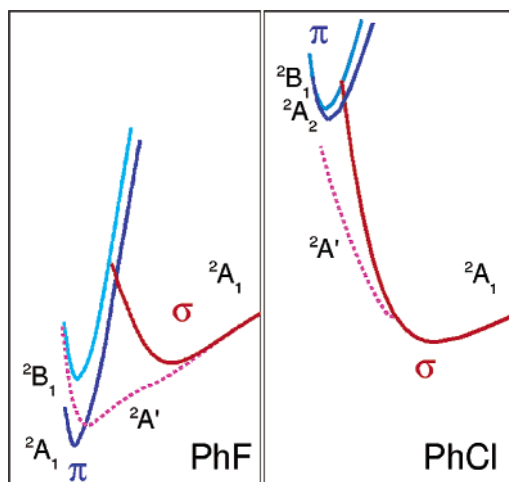
(38) (a) Previous calculations using MP2/6-31G**//UHF/6-31G* found the π RA of PhF 65 kcal/mol stable with respect to the fluoride loss. This value was reported to be sensitive to the basis set (see ref 38b). Although our B3LYP results with the same basis are in close agreement with the informed value, we determined that the energy difference decreases to 21–20 kcal/mol by basis set improvement to 6-31+G* and 6-311+G(2d,p) with the B3LYP functional; this value was also checked at CCSD/6-31+G*//CCD/6-31G* level. (b) Denney, D. B.; Denney, D. Z.; Fenelli, S. P. *Tetrahedron* **1997**, *53*, 9835.

FIGURE 7. Comparisson of the PhF and PhCl RAs on the $\pi-\sigma$ interconversion zone.
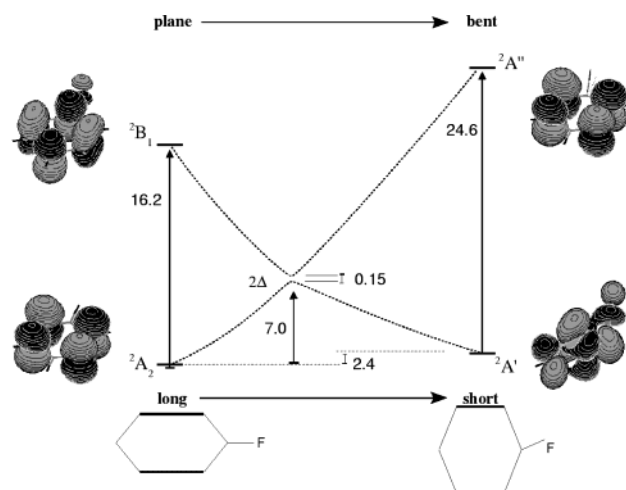

FIGURE 8. CASSCF(9,8) study of interconversion from the $^2A_2$ and the nonplanar $^2A'$ PhF RA species (structures compared in Figure 2b). From the planar $^2A_2$ RA, the most relevant zero order states are those with the a_2 and b_1 π^* orbitals as SOMOs, respectively. All energies in kcal/mol.

distribution mainly located at the ortho and meta positions as expected from the a_2 SOMO. The $^2B_1$ π^* state appears with a vertical gap of 16.2 kcal/mol with respect to the ground.[40] A transition state between the plane and the bent structures (the latter with a weight of 0.93 for the configuration with the b_1 type SOMO) was located with CASSCF(9,8) by searching the crossing point of the $^2A_2$ and the $^2A'$ surfaces. This transition state is similar to that of B3LYP but with a slightly higher barrier (7.0 kcal/mol (Figure 8)).

A similar energy ordering of π states is calculated for PhCl RA; the $^2B_1$ state lies closer to the $^2A_2$ ground than for PhF. The vertical gap found was 10.4 kcal/mol, close to the 11 kcal/mol value deduced from scattering spectra.[28b,d,41] The key difference with PhF arises from

(39) San Roman, E.; Kerbs, P.; Schindewolf, N. *Chem. Phys. Lett.* **1997**, *22*, 84.

(40) This ordering and energy separation is also in agreement with previous theoretical and experimental evidence; the $^2A_2 - {}^2B_1$ energy difference deduced from electron scattering data is 14.1 kcal/mol (ref 28b,d).
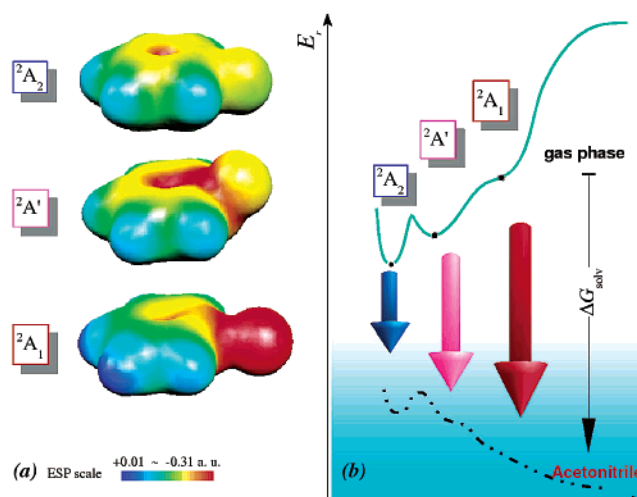
FIGURE 9. (a) The electrostatic potentials for the PhF different anionic species. (b) Solvent stabilization of the gas-phase surfaces (see Table 2).

the considerable thermodynamic instability of these species with respect to the σ surface. The $^2A_2$ structure is very close to the $\pi-\sigma$ crossing,[42] and this instability has been previously proposed.[22a,b]

With relation to the σ surface, the RAs minima were found, by means of all correlated methods used, at C–X of 2.3–3 Å for the different halogens.[43] These slightly bounded $^2A_1$ species have most of the negative charge on the halogen and the radical character on the ipso carbon, with an elongated C–X distance and similar C–C ring bond lengths. These intermediates are not of purely electrostatic nature.[44]

In the gas phase, the PhF $^2A_2$ RA is considerably more stable with respect to the dissociated fragments. However, as schematically shown in Figure 9, the incorporation of MeCN stabilizes the (Ph$^{\bullet}\cdots$F$^-$) surface to a great extent, mainly due to its higher charge localization. The relative energies, evaluated in MeCN with respect to the species in the gas phase, are indicative of the free energy of solvation in this solvent (Table 2).

Thus, in MeCN, the π intermediate cleaves exothermically and the intra-ET becomes the kinetically determining step (see Table 2). For X = Cl, Br, and I, the $\pi-\sigma^*$ intra-ET, exothermic in gas phase, becomes even more exothermic in a polar solvent.

In light of the results here presented, a concerted dissociative mechanism should be the most accessible

(41) This proximity and the a_2 nature of the most stable π RA is also in agreement with spectroscopic data from different sources (refs 8b, 19, 28).

(42) Even though the $^2A_2$ state has all positive frequencies at the HF level and the multiconfigurational studies confirm its ground state nature, the B3LYP structure has a spurious imaginary frequency due to the sharpness of the surface near the highly exothermic $\pi-\sigma$-sigma conversion zone.

(43) Previous PMP2 calculations found this surface without any minima (see ref 22b). However, we have performed different MP levels and CC calculations, as shown in Supporting Information, and for all correlated methods, the σ RA actually appears. On the other hand, at the HF level, the σ surface results strictly dissociative.

(44) Electrostatic complexes generally appear at distances greater than 3 Å in contrast to the σ RAs found between 2.3 and 3 Å for the different halogens. At variance with the RAs, the complexes have practically all the spin density on the ipso carbon and nearly all the extra charge on the halogen, which does not contribute to their SOMO.

pathway for the ET to PhCl, PhBr, and PhI in a polar solvent. The switch to a stepwise pathway, by raising the driving force, cannot be disregarded along the whole series. This possibility, under a set of given conditions, decreases as the σ curve shifts to lower energies with respect to the π curve (see Figure 5b).

There is experimental evidence in agreement with this theoretical trend. The RAs of PhCl and PhBr have been generated electrochemically.[45] Through this technique, a fragmentation rate constant of 4×10^7 s^{-1} has been determined for X = Cl in liquid ammonia[46a] (-38 °C) while it is estimated as diffusion control in DMF, even for X = Cl (at least 6 orders of magnitude faster than the most reactive acetyl derivative).[46b] Recently, it has been shown that a mechanistic change from concerted to stepwise can be achieved for PhI by scan rate modifications while PhBr follows a stepwise mechanism over the whole range of scan rates used.[7h] On the other hand, PhF, the most clearly different species in the family, seems an interesting example to obtain experimental evidence for a stepwise-concerted mechanistic switch in solvents of different polarity.

It is interesting to remark that the presence of two available π states is required in order to understand the stepwise pathway for the peculiar case of the halobenzenes. With enough driving force to reach the $^2A_2$ curve, the RA could be formed. On the other hand, the relative proximity of the $^2B_1$ state effectively assists the $\pi-\sigma$ interconversion even in the less-favored case of PhF, otherwise with a higher $\pi-\sigma$ barrier (see Figure 6). On the contrary, if *only* the $^2B_1$ like species are considered,[47] there should be no reason to justify the intermediacy of radical anions as dissociation from this state does not require an important barrier and it is expected as extremely exothermic in most polar solvents.

Concluding Remarks

The B3LYP functional has been able to reproduce useful parameters by comparing data from both the neutral and anionic potential surfaces with gas-phase properties for the halides and their radical anions; this was possible at a reasonable computational cost, with rather compact basis such as 6-31+G*.

From the DFT results, the expected reactivities of the *p*-nitrochlorobenzene and of the *p*- and *m*-chloroacetophenone, with stable π RAs, are in agreement with their experimental behavior. Apart from the thermodynamic stability of these intermediates, the results demonstrate the importance of the difference in energy between the π and σ curves, their topology, and the geometric and electronic properties of the different anionic species in the rate of fragmentation (consider *m*- vs *p*-chloroacetophenone, which have RAs with similar stabilities). In all cases, the stabilizing effect of a polar solvent is manifested to a greater extent for the σ species and dissociated products. In acetonitrile, most π species can dissociate through an exothermic process once the intra-ET to the σ^* (C$-$X) has occurred. On the other hand, the fragmentation of the most stable *p*-nitrochlorobenzene π RA is still endothermic in solution. However, the reorganization of the charge and spin associated to the $\pi-\sigma$ intra-ET is kinetically important even in this case, since the energy required to release the chloride anion from the solvated σ species is small and the major contribution to the activation barrier in a polar solvent comes from the $\pi-\sigma$ interconversion (Figure 3).

In the particular case of the halobenzenes, the assistance of a second π^* state favors the adiabatic $\pi-\sigma$ interconversion. The role of this π^* state is more relevant for PhF, which has the thermodynamically more stable π RA of the series due to the high energy of the σ^* C$-$F MO. Conversely, for the same π phenyl system and X = Cl, Br, and I, the π RA lies at higher energy than the σ and dissociated species and the possibility of its formation diminishes as the energy of the σ^* C$-$halogen decreases, this for a given set of experimental conditions. In all cases, the $\pi-\sigma$ interconversion turns exothermic due to the stabilizing effect of a polar solvent. On the other hand, the thermodynamics of the dissociation depends also on the solvation energy of each leaving group in a particular solvent.

The calculations presented here allow the rationalization of the experimental behavior of haloaromatic RAs having reactivities that cover a wide range of fragmentation rates.

Supporting Information Available: This material has been arranged in two parts. Part 1 contains, for comparison purposes, a detailed summary of the π and σ RAs obtained for PhCl from different formalisms used in this work. Atomic units, energies, and main geometric parameters up to the CCSD(T)/6-31+G*// CCD/6-31G* level are supplied as Table S1. The parameters indicated in Figure 5, useful to address the quality of the gas-phase anionic surfaces (see text) are compared against experimental data in Table S2. The vertical negative electron affinities are plotted for the halobenzenes against those obtained by electron scattering in Figure S1. Part 2 contains Figures S2$-$S5 that show different potential energy surface profiles for the neutral and anionic curves for PhCl, PhBr, and PhI in gas phase and acetonitrile. Both parts are available as a PDF file. The *xyz* coordinates of the main stationary points discussed are gathered in a single ASCII text file. This material is available free of charge via the Internet at http://pubs.acs.org.

JO035087W

(45) Andrieux, C. P.; Blocman, C.; Dumas-Bouchiat, J. M.; M'Halla, F.; Savéant, J.-M. *J. Am. Chem. Soc.* **1980**, *102*, 3806.

(46) (a) Amatore, C.; Combellas, C.; Pinson, J.; Oturan, M. A.; Robveille, S.; Savéant, J.-M.; Thiébault, A. *J. Am. Chem. Soc.* **1985**, *107*, 4846. (b) Andrieux, C. P.; Blocman, C.; Dumas-Bouchiat, J. M.; Savéant, J.-M. *J. Am. Chem. Soc.* **1979**, *101*, 3431.

(47) In ref 22b, the only anion state taken into consideration for chlorobenzene is the $^2B_1$. We found by means of the same procedure (PMP2/6-31+G*) the $^2A_2$ at lower energy. See also Supporting Information part 1 where the PhCl RAs are compared at different levels of theory.